

Photocreating supercooled spiral-spin states in a multiferroic manganite

Y. M. Sheu,^{1,2,*} N. Ogawa,² Y. Kaneko,² and Y. Tokura^{2,3}

¹*Department of Electrophysics, National Chiao Tung University, Hsinchu 300, Taiwan*

²*RIKEN Center for Emergent Matter Science (CEMS), Wako, Saitama 351-0198, Japan*

³*Department of Applied Physics and Quantum-Phase Electronics Center (QPEC), University of Tokyo, Tokyo 113-8656, Japan*

(Received 16 December 2015; revised manuscript received 24 February 2016; published 18 August 2016)

We demonstrate that the dynamics of the *ab*-spiral-spin order in a magnetoelectric multiferroic $\text{Eu}_{0.55}\text{Y}_{0.45}\text{MnO}_3$ can be unambiguously probed through optical second harmonic signals, generated via spin-induced ferroelectric polarization. In the case of weak excitation, the ferroelectric and the spiral-spin order remains interlocked, both relaxing through spin-lattice relaxation in the nonequilibrium state. When the additional optical pulse illuminating the sample is intense enough to induce a local phase transition thermally, the system creates a metastable state of the *bc*-spiral-spin order (with the electric polarization $P \parallel c$) via supercooling across the first-order phase transition between the *ab* and *bc* spiral. The supercooled state of the *bc*-spiral spin is formed in the thermodynamical ground state of the *ab* spiral ($P \parallel a$), displaying a prolonged lifetime with strong dependence on the magnetic field along the *a* axis. The observed phenomena provide a different paradigm for photoswitching between the two distinct multiferroic states, motivating further research into a direct observation of the photocreating supercooled *bc*-spiral spin in multiferroic manganites.

DOI: [10.1103/PhysRevB.94.081107](https://doi.org/10.1103/PhysRevB.94.081107)

Spin kinetics via light-matter interactions has been of great interest ever since the discovery of ultrafast demagnetization in a ferromagnetic metal [1]. The exchange interaction, spin-orbit interaction, and spin precession are believed to dominate spin relaxation after photoexcitation [2]. The recent development of spin-induced magnetoelectric (ME) multiferroics [3–7] brings up substantial questions about the photoinduced dynamics due to more delicate interactions. ME multiferroics of a spiral-spin origin can lead to cross correlations between ferroelectric (FE) and spiral-spin orders, since the ionic displacement is a direct consequence of the inverse Dzyaloshinskii-Moriya (DM) interaction [8,9]. The spin dynamics of ME multiferroics has been a subject of scrutiny [5,10–13] as it may become the platform for ME memory [14]. Although insight into the dynamical spiral-spin response has been given by using resonance THz or ac electric fields [10–13,15,16], a comprehensive understanding of ME dynamics is still lacking, primarily due to the lack of direct access to the FE order on various time scales [17,18]. However, their influence could be significant and unexpected states might be accessible from couplings between different degrees of freedom (DOF) in nonequilibrium cases. Therefore, we aim to unveil the photoexcited dynamics of spiral-spin-induced ME coupling.

Multiferroic perovskite manganites, $R\text{MnO}_3$ [*R* being Tb, Dy, (Eu,Y), etc.], possess either *ab*- or *bc*-plane spin-spiral states (abbreviated as *ab* spiral and *bc* spiral) with the propagation wave vector *k* along the *b* axis [Fig. 1(a)]. The two spiral states give rise to FE polarization, $P \parallel a$ or $P \parallel c$, respectively, through the inverse DM interaction [8,9,19]. An external magnetic field (*B*) changes the axis of the spin cone, flipping between the *ab* spiral (under $B \parallel c$) and the *bc* spiral (under $B \parallel a$) through a first-order phase transition (1stPT) [20] [Fig. 1(b)].

To explore the photoinduced phenomena of the two distinct ME states in perovskite manganites, we utilize the spin-

induced FE polarization of $\text{Eu}_{0.55}\text{Y}_{0.45}\text{MnO}_3$ (EYMO) to produce second harmonic generation (SHG). SHG has been frequently applied to multiferroics of a spiral-spin origin, such as MnWO_4 [15,21–23], TbMnO_3 [24], TbMn_2O_5 [16], and CuO [25]. The techniques have been reviewed in depth [26,27]. Time-resolved SHG (TR-SHG) can directly access the FE polarization (or, equivalently, the spiral-spin order here), spanning a wide range of time scales [15,28–30]. Time-resolved research is practical for tracing the dynamics of various DOF [6,30–36]. Besides, the capability of generating highly nonequilibrated states with ultrashort pulses may lead to the discovery of hidden states [37–39], which would not be realized through conventional thermodynamic processes.

Single crystals EYMO of orthorhombic perovskite were grown by the floating zone method. The *ac* surface was mechanically polished to ~ 1 mm thickness, and annealed at 750°C in air for 12 h to reduce the residual strain. It was mounted in a cryostat with a superconducting magnet and in contact with exchange He gas, allowing for a significant reduction in cooling time of the sample, especially when heated by laser pulses.

Our TR-SHG experiments are based on an amplified Ti:sapphire laser system (1 kHz and ~ 120 fs centered at 800 nm). Photon energies (E_{ph}) of 0.48–1.12 eV are generated by optical parametric amplifiers. The SHG signal is detected by a photomultiplier tube using lock-in techniques after filtering out the fundamental photon. A combination of an optical chopper and a mechanical shutter is employed for the long-time-delay measurements. All measurements are performed under zero field cooling.

At low temperature (*T*), EYMO has an *ab*-spiral ground state ($P \parallel a$), of which the free-energy landscape is illustrated by the left inset of Fig. 1(b). As *T* rises, the *bc* spiral becomes thermodynamically more stable. The 1stPT between the two spin-spiral states occurs around 21 K, above which the FE polarization rotates to along the *c* axis [20,41]. At 6 K without *B*, the polar plot of *p*-polarized ($\parallel a$) and *s*-polarized ($\parallel c$)

*Corresponding author: ymsheu@nctu.edu.tw

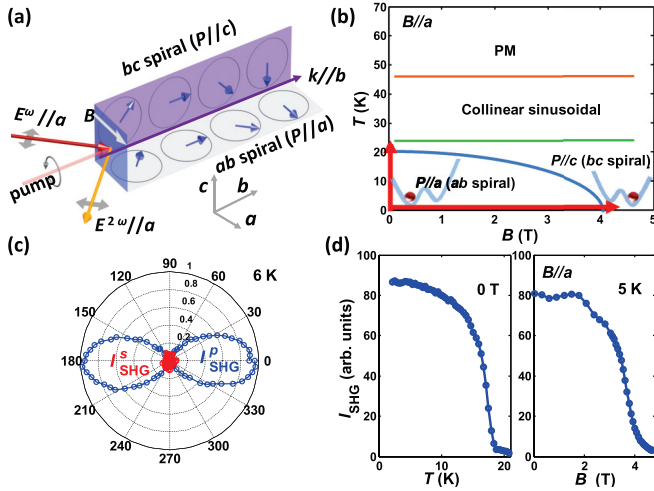


FIG. 1. (a) Schematic illustration for the TR-SHG in a reflection configuration. Incident p (p -in) and s (s -in) photon polarizations correspond to $E^\omega // a$ and $E^\omega // c$. The wave vector k of the ab and bc spiral is along the b axis. (b) Schematic phase diagram ($B // a$) of EYMO reproduced from Refs. [20,40]. The two free-energy landscapes in the inset illustrate the ground state of the ab spiral (left) and the bc spiral (right). (c) Polar plot of the SHG (3.1 eV) intensity measured at 6 K, which detects the ab spiral with $P // a$. I_{SHG}^p and I_{SHG}^s represent the p -polarized (p -out) and s -polarized (s -out) SHG, respectively. (d) Temperature (T) and magnetic field ($B // a$ axis) dependence of the static SHG for the p -in and p -out configuration. The phase transitions from the ab to the bc spiral, observed in (d), are indicated as vertical (through temperature) and horizontal (through B) red arrows in the phase diagram of (b).

SHG is displayed in Fig. 1(c). The polar patterns are consistent with the emergence of FE polarization along the a axis. More details about the SHG-tensor analysis are given in the Supplemental Material [42]. Figure 1(d) shows the p -polarized SHG intensity I_{SHG} vs T (left panel) and $B // a$ (right panel), being consistent with the occurrence of an ab spiral in the phase diagram of Fig. 1(b). It is worth noting that the applied $B // a$ rotates the axis of the spin cone and the FE polarization from $P // a$ to $P // c$, decreasing I_{SHG} and changing the free-energy landscape [right inset of Fig. 1(b)]. The B -dependent SHG clearly identifies the ab spiral through the spin-induced FE polarization. The associated SHG reduction under $B // a$ is a consequence of the bc -spiral formation due to the 1stPT. We note that the bc spiral is not directly detectable by SHG, likely due to the considerably small polarization. A discussion about the missing SHG from $P // c$ is provided in the Supplemental Material [42].

Upon relatively weak photoexcitation ($< 1 \mu\text{J}$; $1 \mu\text{J}$ at 0.77 eV corresponds to 4.24 J/cm^3 in our data), we observe a gradual reduction in I_{SHG} as a function of delay time t [Fig. 2(a)]. The photoinduced depolarization is completed around $t \sim 50$ – 100 ps, and the time constant is independent of T , B , excitation fluence E_{ph} [Figs. 2(a)–2(d)], or light polarization (circular and linear; only the circular is shown). The time constant for I_{SHG} reduction is within the typical range of spin-lattice (S-L) relaxation in manganites [43–45], in accord with a recent report [17] and our transient reflectivity ($\Delta R/R$) data [42]. It is noted that the I_{SHG} for $t < 0$

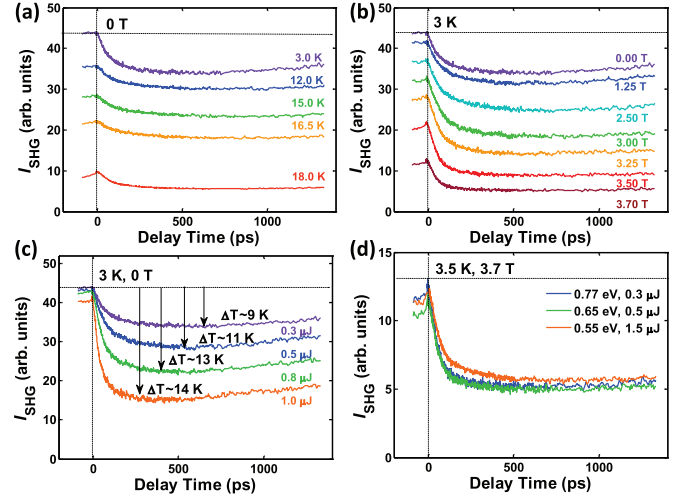


FIG. 2. Spin-lattice relaxation as the origin of TR-SHG response under low excitation ($< 1 \mu\text{J}$). TR-SHG signal of the p -in (1.0 eV) and p -out (2.0 eV) setups [Fig. 1(a)], measured (a) at various T in zero field, (b) in various B at 3 K, and (c) under different excitation intensities at 3 K in zero field. Pump E_{ph} is 0.77 eV. Here, the $1 \mu\text{J}$ excitation corresponds to a $1 \mu\text{J}$ per pulse energy at 1 kHz and energy density 4.24 J/cm^3 . (d) Traces of TR-SHG measured under different E_{ph} 's. The excitation intensity was chosen so as to induce a similar amount of reduction in I_{SHG} to compare the dynamics.

corresponds to the steady-state SHG at 1 ms after an 120 fs pulse excitation and depends on T and $B // a$ [Fig. 1(d)].

Comparing our $\Delta R/R$ with TR-SHG [42], we can conclude that TR-SHG unambiguously probes the spiral-spin dynamics without an electronic contribution to the FE depolarization, due to the lack of a fast electronic response < 1 ps in TR-SHG, while it is discerned in $\Delta R/R$. Besides, the insensitivity of TR-SHG to pump E_{ph} again implies that the relaxation of spiral spin is not triggered by an electronic contribution from specific optical transitions (including the d - d transition here and the p - d charge transfer [17]). We can infer that the local spins (of t_{2g} electrons) are still responsible for the FE polarization after an electronic transition and/or transfer of excited e_g electrons, maintaining FE and spin interlock in the nonequilibrium case. Further insights beyond the scope of this Rapid Communication are provided in the Supplemental Material [42].

The lack of an electronic response and the characteristic S-L time constant observed in TR-SHG implies thermal-induced spin depolarization upon photoexcitation. The transient and quasiequilibrium lattice temperature can be deduced from the TR-SHG traces at various T 's [Fig. 2(a)]. At 3 K, using $0.3 \mu\text{J}$ pulses ($E_{ph} = 0.77$ eV), the estimated change in T (ΔT) is ~ 9 K from the reduced magnitude of I_{SHG} . At a fixed fluence, ΔT reduces with increasing the sample base temperature [Fig. 2(a)], whereas it stays constant upon changing the magnitude of $B // a$ [Fig. 2(b)]. This is reasonably anticipated from the increase of heat capacity at higher T . The time constant for the laser-induced-heating process does not depend on the E_{ph} ranging from 0.55 to 1.55 eV [Fig. 2(d)]. Furthermore, the insignificant change in relaxation time near the transition indicates the nature of 1stPT, unlike

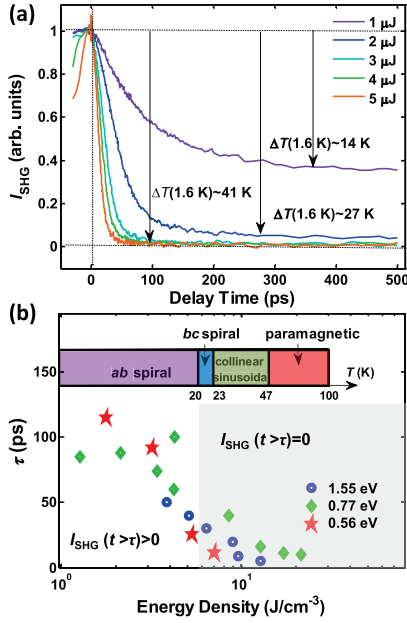


FIG. 3. Formation of metastable states under high excitation. (a) TR-SHG of *p*-in (1.0 eV) and *p*-out (2.0 eV) setups measured at 1.6 K under various pump intensities ($> 1 \mu\text{J}$). The vertical arrows indicate the estimated change in lattice temperature. (b) Time constant of FE depolarization vs excitation energy density at three E_{ph} 's. The time constant is extracted from the fit of a single exponential decay. The shaded gray area covers the excitation density leading to the complete reduction of the SHG (i.e., phase transition to the *bc* spiral or higher- T phases). The color blocks in the inset represent the corresponding lattice temperatures and the respective multiferroic/magnetic phases therein.

the critical behavior of spin kinetics in manganites that possess second-order phase transitions [44–46].

Intriguing phenomena are uncovered as the excitation density increases further: Photodepolarization of the spin-induced FE becomes faster and finally the I_{SHG} disappears completely [Fig. 3(a)]. To discern its origin, we plot the decay time constant versus excitation energy density in Fig. 3(b), revealing a threshold behavior irrespective of pump E_{ph} . Above the threshold the TR-SHG goes to zero within 20 ps and remains at zero for a long time (> 500 ps), whereas below the threshold TR-SHG never completely reduces to zero, and slow S-L relaxation dominates the FE depolarization, irrespective of sample temperature and magnetic field. Thus the threshold energy density differentiates the “low” and “high” excitation regime, illustrated in the white and gray area of Fig. 3(b). The correlation with pump energy density and the irrelevance of pump E_{ph} makes the TR-SHG an ideal thermometer for the nonequilibrium spin subsystem in a low-excitation case, allowing us to determine the transient spin temperature. In the high-excitation case, we can estimate the lattice temperature [inset of Fig. 3(b)] by linear extrapolation since the $I_{\text{SHG}}(t)$ disappears completely and no longer works as a spin thermometer. We find that once the transient temperature ($T + \Delta T$) is above T_c of the *ab* spiral, the I_{SHG} decreases faster and disappears completely for a prolonged time (> 500 ps).

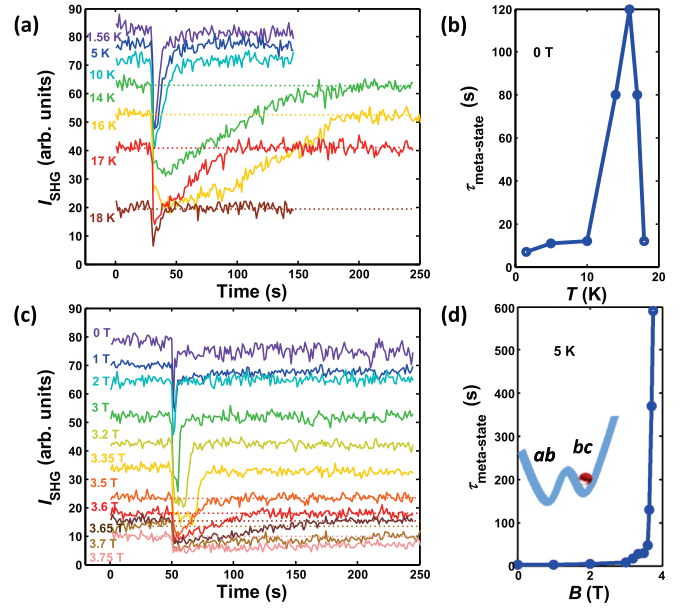


FIG. 4. Photocreating the metastable *bc* spiral from the ground state of the *ab* spiral. The high excitation in the gray area of Fig. 3(b) creates a metastable spin state, which is probed by the long-lived reduction in spin-induced SHG: (a) TR-SHG measured at various temperatures and (b) the corresponding lifetimes of the metastable states. (c) The recovery of photocreating metastable states under application of various $B \parallel a$ at 5 K, and (d) the corresponding lifetimes. The inset illustrates a schematic free-energy landscape against the canting angle of the spin-spiral plane around the *b* axis and a formation of the metastable *bc* spiral.

As the pump intensity approaches the threshold, a subtle behavior occurs before $t = 0$ [Fig. 2(c)]. We notice a small reduction of I_{SHG} , which becomes significant under high excitation [Fig. 3(a)], e.g., $I_{\text{SHG}}^{1 \mu\text{J}}(t < 0) < I_{\text{SHG}}^{0.3 \mu\text{J}}(t < 0)$, indicating incomplete recovery of the *ab* spiral within 1 ms and signaling a situation generally not explored in time-resolved optical experiments. The observed reduction is not simply attributable to accumulated lattice thermalization, but rather points to the emergence of metastable spin orders, as discussed below.

To investigate the subtle SHG reduction before $t = 0$ (i.e., existing at 1 ms after photoexcitation), we reduced the pump repetition rate to allow the system to recover the thermodynamical ground state (*ab* spiral) at the base temperature. We also adjust the pump intensity around 24–28 μJ to unveil the dynamics of the metastable state. The resultant SHG traces at various T 's [Fig. 4(a)] and under different $B \parallel a$ [Fig. 4(b)] reveal a dramatic change in the recovery time, spanning from a few seconds up to several minutes. As the base temperature approaches the phase transition, the recovery time becomes longer [Fig. 4(a)]. Similarly, the application of $B \parallel a$ lengthens the recovery time [Fig. 4(b)]. We thus exclude the lattice residual heating as the origin of SHG reduction, since it would not have a strong dependence on the base temperature nor the applied B field. Because $B \parallel a$ energetically favors the *bc* spiral and the (thermal) recovery inevitably goes through the phase of the *bc* spiral, the prolonged response after the intense excitation likely involves the transition of the photogenerated *bc* spiral to the original *ab* spiral.

The remarkably long time scale observed here indicates the formation of a metastable state, reachable by supercooling the system through 1stPT, from which a system cannot escape at low enough temperatures due to the high free-energy potential barrier [47,48]. In other words, the supercooled state preserves partially or dominantly the order of high-temperature states, because the time scale to form the critical size of the thermodynamical ground state becomes long enough. We can estimate the cooling rate from the trace of $1 \mu\text{J}$ excitation shown in Fig. 2(c). The residual heating of $\sim 4 \text{ K}$ is estimated by the SHG signal just before $t = 0$, while the transiently elevated temperature ΔT ($t > 100 \text{ ps}$) is $\sim 14 \text{ K}$, implying a cooling rate as high as 10^4 K/s (10 K recovered in 1 ms). The supercooling is often observed in temperature- and/or magnetic-field-hysteresis features of other multiferroics of RMnO_3 [49] and charge-ordered manganites with 1stPTs [50].

We can use this estimate to differentiate between the two processes of SHG reduction, i.e., lattice heating versus the formation of the metastable state. Using a linear extrapolation of the relation between light absorption and heat for the present experimental condition in Fig. 4, we estimate the lattice heating up to $\sim 300 \text{ K}$ which cools to the base temperature in $\sim 30 \text{ ms}$ after photoexcitation. Here, we neglect the slowdown of thermal transport due to the subsequent heat conduction between interfaces, as our sample is mounted in contact with He exchange gas to achieve better heat relaxation. The recovery time, shown in Figs. 4(b) and 4(d), is nearly four orders of magnitude longer than the lattice cooling time; thus the magnetically ordered phase (e.g., spin spiral) should be restored. We exclude a change in the recovery time arising from the variation in heat diffusion. If it were the case, we would observe a gigantic critical slowing down during S-L relaxation in the low-excitation case [Figs. 2(a) and 2(c)]. Instead, the prolonged SHG recovery can be explained in terms of the trap of the bc spiral in the free-energy potential well [inset of Fig. 4(d)], frozen by supercooling. Compared with typical time scales of tens of milliseconds for nucleation and domain growth upon fast electrical poling to induce a spiral-spin flip [15,51], cooling from the upper temperature of the bc spiral to temperatures possessing the thermodynamical ground state of the ab spiral takes less than 1 ms, which is too short to form a large size of the ab -spiral domain. As for the origin of these minima of the free-energy potential well, it could be the high-temperature collinear spin state or some other states. However, during supercooling across the T_c of the bc

spiral, the application of $B \parallel a$ can energetically favor the bc spiral to be trapped momentarily as the transient state. Further cooling can barely overcome the potential barrier between the ab and bc spiral, and the field activated stable phase of the bc spiral cools down and is fixed by the barrier, forming a metastable state at the base temperature [inset of Fig. 4(d)]. Therefore, when the sample is near T_c or under $B \parallel a$, the bc spiral is dominant more than other collinear sinusoidal or disorder states during supercooling. Future investigations of the photocreated supercooled state from a direct bc -spiral signal may help to gain deeper insight. Finally, we note that within the model of the supercooled bc spiral, the peaklike feature near $t = 0$ for excitation $> 4 \mu\text{J}$ in Fig. 3(a) could be understood as repumping the thermodynamically unfavorable metastable state at 1 kHz. Complicated mixtures of excitation could be involved. Experimentally, it disappears upon reducing the laser repetition rate.

In conclusion, by probing the temporal variation of SHG from the spiral-spin-induced FE polarization, we have investigated the dynamics of photoexcited multiferroic EYMO, spanning a time scale from 10^{-12} to 10^3 s . We confirm that there is no specific electronic contribution to FE depolarization apart from the thermalization due to spin-lattice relaxation on all time scales. We find that a metastable bc spiral ($P \parallel c$) can be photocreated from the ab spiral ($P \parallel a$) through supercooling from the photothermalized state. We observe the two distinct dynamics differentiated by a threshold energy density of photoexcitation: Below the threshold the spiral spin relaxes through S-L coupling and the whole system cools back to the base temperature while preserving $P \parallel a$. Contrarily, above the threshold, we observe a remarkably slow SHG recovery with a strong dependence on temperature and magnetic field along the a axis. This feature, together with the estimated cooling rate, allows us to conclude that the formation of the metastable bc spiral ($P \parallel c$) is feasible through supercooling multiferroic manganites upon femtosecond-laser excitation. Our study provides deep insight into the switch of multiferroics of a spiral-spin origin and will pave a different avenue toward nonvolatile memory-storage functionality [39].

The authors thank F. Kagawa for stimulating discussions and M. Ishida for technical help. This research is granted by the JSPS Grant-in-Aid for Scientific Research(S) No. 24224009. Y.M.S. acknowledge the support from the Taiwan Ministry of Science and Technology, Grant No. MOST 104-2112-M-009-023-MY3.

-
- [1] E. Beaupaire, J.-C. Merle, A. Daunois, and J.-Y. Bigot, *Phys. Rev. Lett.* **76**, 4250 (1996).
 [2] A. Kirilyuk, A. V. Kimel, and T. Rasing, *Rev. Mod. Phys.* **82**, 2731 (2010).
 [3] Y. Tokura, *Science* **312**, 1481 (2006).
 [4] W. Eerenstein, N. D. Mathur, and J. F. Scott, *Nature (London)* **442**, 759 (2006).
 [5] S.-W. Cheong and M. Mostovoy, *Nat. Mater.* **6**, 13 (2007).
 [6] M. Fiebig, N. P. Duong, T. Satoh, B. B. Van Aken, K. Miyano, Y. Tomioka, and Y. Tokura, *J. Phys. D: Appl. Phys.* **41**, 164005 (2008).
 [7] Y. Tokura, S. Seki, and N. Nagaosa, *Rep. Prog. Phys.* **77**, 076501 (2014).
 [8] H. Katsura, N. Nagaosa, and A. V. Balatsky, *Phys. Rev. Lett.* **95**, 057205 (2005).
 [9] M. Mostovoy, *Phys. Rev. Lett.* **96**, 067601 (2006).
 [10] A. Pimenov, A. A. Mukhin, V. Y. Ivanov, V. D. Travkin, A. M. Balbashov, and A. Loidl, *Nat. Phys.* **2**, 97 (2006).
 [11] D. Senff, P. Link, K. Hradil, A. Hiess, L. P. Regnault, Y. Sidis, N. Aliouane, D. N. Argyriou, and M. Braden, *Phys. Rev. Lett.* **98**, 137206 (2007).

- [12] A. B. Sushkov, R. V. Aguilar, S. Park, S.-W. Cheong, and H. D. Drew, *Phys. Rev. Lett.* **98**, 027202 (2007).
- [13] Y. Takahashi, R. Shimano, Y. Kaneko, H. Murakawa, and Y. Tokura, *Nat. Phys.* **8**, 121 (2012).
- [14] M. Bibes and A. Barthelemy, *Nat. Mater.* **7**, 425 (2008).
- [15] T. Hoffmann, P. Thielen, P. Becker, L. Bohatý, and M. Fiebig, *Phys. Rev. B* **84**, 184404 (2011).
- [16] T. Lottermoser, D. Meier, R. V. Pisarev, and M. Fiebig, *Phys. Rev. B* **80**, 100101 (2009).
- [17] D. Talbayev, J. Lee, S. A. Trugman, C. L. Zhang, S. W. Cheong, R. D. Averitt, A. J. Taylor, and R. P. Prasankumar, *Phys. Rev. B* **91**, 064420 (2015).
- [18] J. A. Johnson, T. Kubacka, M. C. Hoffmann, C. Vicario, S. de Jong, P. Beaud, S. Grubel, S. W. Huang, L. Huber, Y. W. Windsor, E. M. Bothschafter, L. Rettig, M. Ramakrishnan, A. Alberca, L. Patthey, Y. D. Chuang, J. J. Turner, G. L. Dakovski, W. S. Lee, M. P. Minitti, W. Schlotter, R. G. Moore, C. P. Hauri, S. M. Koochpayeh, V. Scagnoli, G. Ingold, S. L. Johnson, and U. Staub, *Phys. Rev. B* **92**, 184429 (2015).
- [19] I. A. Sergienko and E. Dagotto, *Phys. Rev. B* **73**, 094434 (2006).
- [20] H. Murakawa, Y. Onose, F. Kagawa, S. Ishiwata, Y. Kaneko, and Y. Tokura, *Phys. Rev. Lett.* **101**, 197207 (2008).
- [21] D. Meier, M. Maringer, T. Lottermoser, P. Becker, L. Bohatý, and M. Fiebig, *Phys. Rev. Lett.* **102**, 107202 (2009).
- [22] D. Meier, N. Leo, M. Maringer, T. Lottermoser, M. Fiebig, P. Becker, and L. Bohatý, *Phys. Rev. B* **80**, 224420 (2009).
- [23] D. Meier, N. Leo, G. Yuan, T. Lottermoser, M. Fiebig, P. Becker, and L. Bohatý, *Phys. Rev. B* **82**, 155112 (2010).
- [24] M. Matsubara, S. Manz, M. Mochizuki, T. Kubacka, A. Iyama, N. Aliouane, T. Kimura, S. L. Johnson, D. Meier, and M. Fiebig, *Science* **348**, 1112 (2015).
- [25] T. Hoffmann, K. Kimura, T. Kimura, and M. Fiebig, *J. Phys. Soc. Jpn.* **81**, 124714 (2012).
- [26] M. Fiebig, V. V. Pavlov, and R. V. Pisarev, *J. Opt. Soc. Am. B* **22**, 96 (2005).
- [27] S. A. Denev, T. T. A. Lummen, E. Barnes, A. Kumar, and V. Gopalan, *J. Am. Ceram. Soc.* **94**, 2699 (2011).
- [28] Y. M. Sheu, S. A. Trugman, L. Yan, C. P. Chuu, Z. Bi, Q. X. Jia, A. J. Taylor, and R. P. Prasankumar, *Phys. Rev. B* **88**, 020101 (2013).
- [29] Y. M. Sheu, S. A. Trugman, L. Yan, Q. X. Jia, A. J. Taylor, and R. P. Prasankumar, *Nat. Commun.* **5**, 5832 (2014).
- [30] M. Matsubara, Y. Kaneko, J.-P. He, H. Okamoto, and Y. Tokura, *Phys. Rev. B* **79**, 140411 (2009).
- [31] Y. M. Sheu, S. A. Trugman, Y.-S. Park, S. Lee, H. T. Yi, S.-W. Cheong, Q. X. Jia, A. J. Taylor, and R. P. Prasankumar, *Appl. Phys. Lett.* **100**, 242904 (2012).
- [32] H. Wen, P. Chen, M. P. Cosgriff, D. A. Walko, J. H. Lee, C. Adamo, R. D. Schaller, J. F. Ihlefeld, E. M. Dufresne, D. G. Schlom, P. G. Evans, J. W. Freeland, and Y. Li, *Phys. Rev. Lett.* **110**, 037601 (2013).
- [33] N. Ogawa, T. Satoh, Y. Ogimoto, and K. Miyano, *Phys. Rev. B* **80**, 241104 (2009).
- [34] N. Ogawa, Y. Ogimoto, and K. Miyano, *Appl. Phys. Lett.* **102**, 251911 (2013).
- [35] Y. M. Sheu, S. A. Trugman, L. Yan, J. Qi, Q. X. Jia, A. J. Taylor, and R. P. Prasankumar, *Phys. Rev. X* **4**, 021001 (2014).
- [36] T. Li, A. Patz, L. Mouchliadis, J. Yan, T. A. Lograsso, I. E. Perakis, and J. Wang, *Nature (London)* **496**, 69 (2013).
- [37] H. Ichikawa *et al.*, *Nat. Mater.* **10**, 101 (2011).
- [38] L. Stojchevska, I. Vaskivskyi, T. Mertelj, P. Kusar, D. Svetin, S. Brazovskii, and D. Mihailovic, *Science* **344**, 177 (2014).
- [39] H. Oike, F. Kagawa, N. Ogawa, A. Ueda, H. Mori, M. Kawasaki, and Y. Tokura, *Phys. Rev. B* **91**, 041101 (2015).
- [40] Y. Yamasaki, S. Miyasaka, T. Goto, H. Sagayama, T. Arima, and Y. Tokura, *Phys. Rev. B* **76**, 184418 (2007).
- [41] Y. Takahashi, Y. Yamasaki, N. Kida, Y. Kaneko, T. Arima, R. Shimano, and Y. Tokura, *Phys. Rev. B* **79**, 214431 (2009).
- [42] See Supplemental Material at <http://link.aps.org/supplemental/10.1103/PhysRevB.94.081107> for additional information, including the SHG-tensor analysis, the reasoning for the missing SHG signal of $P \parallel c$, and the comparison between transient reflectivity and TR-SHG in EYMO.
- [43] R. D. Averitt and A. J. Taylor, *J. Phys.: Condens. Matter* **14**, R1357 (2002).
- [44] T. Ogasawara, M. Matsubara, Y. Tomioka, M. Kuwata-Gonokami, H. Okamoto, and Y. Tokura, *Phys. Rev. B* **68**, 180407 (2003).
- [45] G. M. Muller *et al.*, *Nat. Mater.* **8**, 56 (2009).
- [46] R. D. Averitt, A. I. Lobad, C. Kwon, S. A. Trugman, V. K. Thorsmolle, and A. J. Taylor, *Phys. Rev. Lett.* **87**, 017401 (2001).
- [47] A. Barrat, R. Burioni, and M. Mzard, *J. Phys. A* **29**, L81 (1996).
- [48] L. Berthier and G. Biroli, *Rev. Mod. Phys.* **83**, 587 (2011).
- [49] T. Kimura, G. Lawes, T. Goto, Y. Tokura, and A. P. Ramirez, *Phys. Rev. B* **71**, 224425 (2005).
- [50] Y. Tokura, *Rep. Prog. Phys.* **69**, 797 (2006).
- [51] M. Baum, J. Leist, T. Finger, K. Schmalzl, A. Hiess, L. P. Regnault, P. Becker, L. Bohatý, G. Eckold, and M. Braden, *Phys. Rev. B* **89**, 144406 (2014).